

6 The Longitudinal Structure Function F_L at an EIC

Elke C. Aschenauer, Ramiro Debbe, Marco Stratmann

Physics Department, Brookhaven National Laboratory, Upton, New York, USA

6.1 Motivation and Current Status of F_L Results

The DIS reduced cross section σ_r for photon-exchange can be represented as the sum of two independent structure functions F_2 and F_L as follows

$$\sigma_r \equiv \frac{Q^4 x}{2\pi\alpha_{em}^2 Y_+} \frac{d^2\sigma}{dx dQ^2} = F_2(x, Q^2) - \frac{y^2}{Y_+} F_L(x, Q^2) \quad (5)$$

where $Y_+ \equiv 1 + (1 - y)^2$ depends on the inelasticity $y = Q^2/(sx)$ of the process.

F_L is proportional to the cross section for probing the proton with a longitudinally polarized virtual photon and vanishes in the naive Quark Parton Model due to helicity conservation. Starting from $\mathcal{O}(\alpha_s)$, the longitudinal structure function differs from zero, receiving contributions from both quarks and gluons.

At low x , the gluon contribution due to photon-gluon fusion greatly exceeds the quark contribution. Therefore, measuring F_L provides a rather direct way of studying the gluon density and QCD dynamics at small x , i.e., the transition to the high parton density regime. Measurements can be used to test several phenomenological and QCD models describing the low x behavior of the DIS cross section, including color dipole models [89, 90, 91] and expectations from DGLAP fits performed at NLO and NNLO accuracy of QCD. Possible deviations from the DGLAP behavior in the small x , low Q^2 region can be studied by varying kinematic cuts to the data used in the fits.

The longitudinal structure function, or the equivalent cross section ratio $R = \sigma_L/\sigma_T = F_L/(F_2 - F_L)$, was first measured in fixed target experiments and found to be small at large x , $x \geq 0.01$, see, e.g., Ref. [92]. H1 [30] and ZEUS [93] have recently combined their measurements of σ_r for three different proton beam energies [36], $E_p = 920, 575$, and 460 GeV, see Fig 5 in Sec. 3. The extracted F_L , shown in Fig. 12, covers a wide kinematic range, spanning $2.5 < Q^2 < 800 \text{ GeV}^2$ and $0.0006 < x < 0.0036$. As can be seen, F_L is clearly non-zero, and there is some mild tension with the HERAPDF1.0 DGLAP fit [33] at the lowest values of x and Q^2 where one expects non-linear effects to be relevant; see the Chapter on eA physics. In this regime, predictions from the dipole model provide a better description of the data. However, the achieved statistical precision of the combined H1 and ZEUS measurement is too limited to be conclusive.

6.2 Measurement Strategy and Experimental Challenges

The measurement of F_L relies on an accurate determination of the variation of the reduced cross section (5) for common values of the (x, Q^2) bin centers at different beam energies, i.e., c.m.s. energies \sqrt{s} . Relative normalizations and systematic uncertainties of the different data sets for σ_r have to be well under control.

F_L and F_2 can be extracted simultaneously from σ_r by plotting σ_r for fixed values of (x, Q^2) as a function of y^2/Y_+ . F_L is then determined as the slope of the line fitted to the

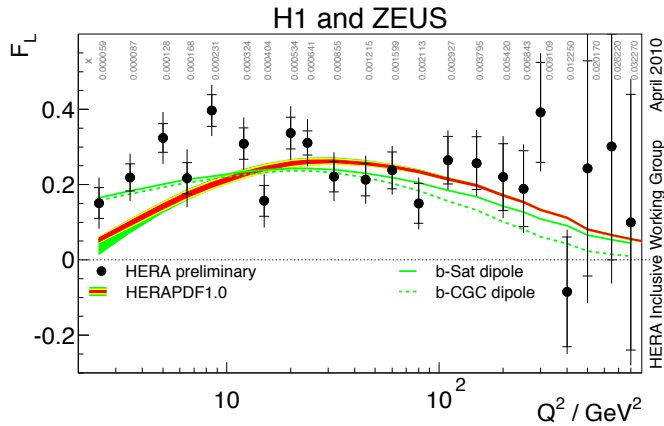


Figure 12: Combined H1 and ZEUS extraction of F_L [36] as a function of Q^2 averaged over x compared to the HERAPDF1.0 fit and predictions from dipole models.

measurements of σ_r for different values of \sqrt{s} : $F_L(x, Q^2) = -\partial\sigma_r(x, Q^2, y)/\partial(y^2/Y_+)$. Likewise, F_2 is the intercept of the fitted line with the y axis: $F_2(x, Q^2) = \sigma_r(x, Q^2, y = 0)$. All measurements at HERA are observed to be consistent with the expected linear dependence [30, 93, 36]. At any given value of Q^2 , the lowest possible x values are only accessed by the highest \sqrt{s} , and the slope related to F_L cannot be determined. Hence, the Rosenbluth separation limits the kinematic coverage of F_L at small x . At larger values of x , measurements of σ_r for various different \sqrt{s} are available and the slopes can be straightforwardly extracted.

The contribution of F_L to the reduced cross section (5) can be sizable only at large values of y . For low values of y , σ_r is very well approximated by the structure function F_2 [30, 93, 36]. Low y data can be used to normalize data sets taken at different c.m.s. energies relative to each other. For measurements at high y the reconstruction of the DIS kinematics using the scattered lepton, the so called “electron method”, has the best resolution and was used at HERA.

In the large y region, $y \gtrsim 0.5$, and low x the electron method is prone to large QED radiative corrections which can reach a level of more than 50% of the Born cross section. Studies based on the DJANGO [94] and HECTOR [95] programs for HERA kinematics show that the largest radiative contributions arise because of hard initial-state radiation (ISR) from the incoming lepton [30]. The radiated photon usually escapes in the beam pipe and the $E - P_z$ of the event is reduced. Therefore, hard ISR can be efficiently suppressed to a level of about 10% at HERA with only a slight residual dependence on y by requiring $E - P_z$ close to the nominal value of twice the electron beam energy implied by energy-momentum conservation [30]. $E - P_z$ can be reconstructed from the measured final-state particles. At the highest y , $y \gtrsim 0.7$, corrections increase due to QED Compton events which can be rejected by certain topological cuts. All cross section measurements at HERA are corrected for QED radiation up to $\mathcal{O}(\alpha_{em})$ using HERACLES [96] which is included in the DJANGO package; further details can be found in Sec. XX.

Kinematically, for low Q^2 , large values of y correspond to low energies of the scattered lepton. Selecting high y events is thus further complicated due to a possibly large background from energy deposits of hadronic final state particles leading to fake electron signals. However, the cut on $E - P_z$ also suppresses such type of backgrounds. In addition, electron tracking, which is foreseen for an EIC detector, will largely eliminate fake electron signals as an additional cut on $E/p \simeq 1$ can be placed to identify the lepton.

Extractions of F_L are certainly the most demanding inclusive structure function measurements but an EIC will have many advantages compared to HERA, in particular, the

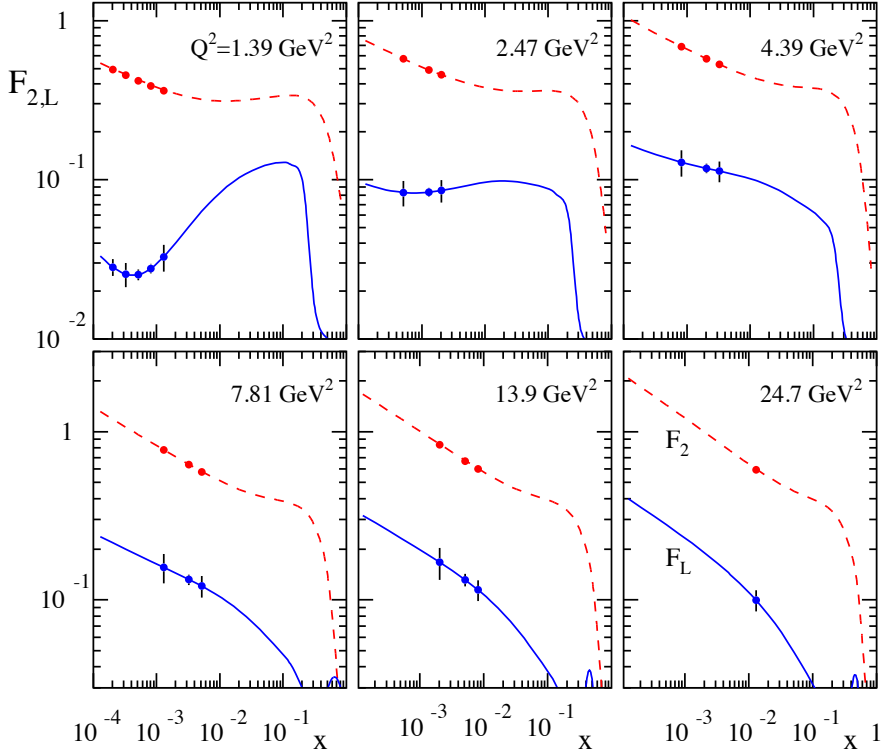


Figure 13: Projected uncertainties for an extraction of F_2 and F_L from a Rosenbluth separation for data taken at three different c.m.s. energies. Also shown are theoretical expectations at NNLO based on the ABKM09 set of PDFs [19] (see text).

possibility to vary \sqrt{s} in a wide range for high luminosity collisions. Also, much better detector capabilities, for instance, concerning the electron, are foreseen. One can also take advantage of all the analysis techniques and Monte Carlo codes developed for HERA to deal with QED radiative corrections.

6.3 Expectations for the EIC

Pseudo-data for the reduced cross section (5) have been generated using the Monte Carlo generator LEPTO [97] for the first stage of an EIC (5 GeV electrons on 100, 250, and 325 GeV protons). The CTEQ6L set of PDFs [87] has been used in the simulations. The hadronic final state was simulated using JETSET [86]. We note that the current pseudo-data do not include any simulations of QED radiative effects and reflect statistical uncertainties which could be achieved by running one month at each of the beam energy settings with the projected luminosities for eRHIC. In addition, a 1% systematic uncertainty is added.

Figure 13 shows the structure functions F_L and F_2 extracted from the pseudo-data of the reduced cross section by means of a Rosenbluth separation, requiring a minimum scattered lepton momentum of 0.5 GeV, $Q^2 > 1 \text{ GeV}^2$, $0.01 < y < 0.90$, and $0.5^\circ < \theta < 179.5^\circ$. To guide the eye, the expected uncertainties are placed on theoretical expectations for $F_{2,L}$ at NNLO accuracy using the ABKM09 set of PDFs [19]. One should note that these PDFs use only data with $Q^2 > 2.5 \text{ GeV}^2$ in their fit and, hence, the behavior of $F_{2,L}$ in the lowest Q^2 bin must be taken with a grain of salt and are only for illustration. The extracted uncertainties take detector smearing of the scattered electron momentum into account. The

momentum resolution was taken from ZEUS, i.e., $\delta p/p = 0.85\% + 0.25\% \times p$.

6.4 Summary and To-Do Items

Like for most inclusive and semi-inclusive measurements at the EIC, an extraction of F_L will be dominated by systematic uncertainties which need to be thoroughly addressed. This is work in progress. It is planned to study the unfolding of F_L in great detail both in ep and eA scattering, including QED radiative corrections and a full simulation of the detector. This will elucidate to what extent the methods developed and used at HERA [30, 93, 36] are suited for high precision measurements of F_L aimed at the EIC. In any case, it will be crucial to design the relevant detector components very carefully to optimize

- the luminosity measurement and its relative calibration for running at different c.m.s. energies,
- the lowest lepton momentum we can detect (0.5 GeV would be desirable),
- the identification of the scattered lepton to suppress potential background from misidentified hadrons,
- the resolution in momentum and scattering angle of the scattered lepton, and
- the acceptance for the hadronic final state to suppress events which have a photon radiated from the incoming or outgoing lepton as well as quasi real photo-production events.

Details on the design of the detector are given in Sec. ???. Also, it will be possible to extract F_L from the EIC data alone, but the combination of the EIC reduced cross section measurements with the ones from HERA may provide an even better lever arm in a larger x, Q^2 range. This needs to be investigated.

Finally, we note that even for statistically very precise measurements of σ_r , the Rosenbluth separation of F_L , i.e., the determination of the slope with respect to y^2/Y_+ , can lead to significantly larger uncertainties if the measured values of σ_r have very similar y^2/Y_+ . This source of uncertainties needs to be minimized by optimizing the binning in y and the set of different c.m.s. energies \sqrt{s} . Studies in this direction are ongoing as well.